

Unambiguous observation of subband transitions from longitudinal valley and oblique valleys in IV–VI multiple quantum wells

H. Z. Wu^{a)}

School of Electrical and Computer Engineering and Laboratory for Electronic Properties of Materials, University of Oklahoma, Norman, Oklahoma 73019

N. Dai and M. B. Johnson

Department of Physics and Astronomy and Laboratory for Electronic Properties of Materials, University of Oklahoma, Norman, Oklahoma 73019

P. J. McCann and Z. S. Shi

School of Electrical and Computer Engineering and Laboratory for Electronic Properties of Materials, University of Oklahoma, Norman, Oklahoma 73019

(Received 6 November 2000; accepted for publication 9 February 2001)

PbSe/PbSrSe multiple-quantum-well (MQW) structures were grown on BaF₂(111) substrates by molecular-beam epitaxy and characterized by Fourier transform infrared transmission spectroscopy. To reduce unwanted Fabry–Pérot interference fringes, the top surface of the MQW samples was coated with an anti-interference film, enabling clear observation of subband transitions without superposed interference fringes. Transition energies involving longitudinal and oblique valleys were unambiguously resolved and are in good agreement with calculations made using the envelope wave function approximation. © 2001 American Institute of Physics. [DOI: 10.1063/1.1361104]

Quantum wells and superlattices based on IV–VI lead chalcogenide semiconductor materials, such as PbSe/PbSrSe or PbTe/PbEuTe, are useful for the fabrication of midinfrared laser diodes and detectors.^{1–5} IV–VI semiconductors have several advantages over narrow gap III–V semiconductors for device fabrication. Symmetric band structures, i.e., holes in IV–VI materials such as PbSe have effective masses just as small as electrons, as evidenced by similar carrier mobilities in both *n*-type and *p*-type materials,⁶ and the absence of a degenerate heavy hole band, which reduces Auger recombination, allow stimulated emission at relatively low generation rates. The recent observation of room temperature continuous wave (cw) photoluminescence from IV–VI multiple-quantum wells (MQWs) using low power density diode laser pumping provides evidence of these properties.⁷ Several groups using different optical techniques have studied the electronic band structures of IV–VI MQW structures. Ishida *et al.*⁸ measured infrared transmission through PbTe/PbEuTe MQW layer structures grown on (100)-oriented KCl substrates, and absorption edges corresponding to *n* = 1, 2, 3, and 4 subband transitions were observed in a sample with 30 nm thick PbTe QWs. More recently, Yuan *et al.*⁹ performed Fourier transform infrared (FTIR) transmission spectroscopy measurements on similar PbTe/PbEuTe MQW structures, but grown on (111)-oriented BaF₂ substrates. Spectral fitting calculations using the Kramers–Kronig relationship yielded an absorption spectrum for a sample with 6.2 nm thick PbTe QWs at 77 K, and three absorption edges at 250, 306, and 327 meV were revealed. These additional subband transitions can be explained by considering the electronic band structure of IV–VI semiconductors. The direct band gap is at the four equivalent *L* points in the Brillouin zone, so for

MQW structures grown on (111)-oriented substrates one *L* valley is normal to the substrate surface, and the other three are at oblique angles. Two different effective masses thus exist for potential variation along the [111] direction, as is the case for MQW layers grown on BaF₂(111), one for the three oblique (*o*) valleys $m_{111}^{\text{oblique}} = 9m_l m_t / (8m_l + m_t)$ and one for the single longitudinal (*l*) valley $m_{111}^{\text{longitudinal}} = m_l$, where m_l and m_t are the longitudinal and transverse effective masses, respectively, associated with the prolate ellipsoids of revolution that define the constant energy surfaces for electrons and holes in IV–VI materials.¹⁰ Thus for PbSe QWs grown on a (111)-oriented substrate, the quantum size effect will remove *L*-valley degeneracy placing the longitudinal valley (normal to the substrate surface) at a lower energy than the three degenerate oblique valleys. However, this theoretical prediction has not been clearly observed by optical spectroscopies^{7–9} because of the superposition of strong interference fringes on the subband transitions. As part of an effort to further investigate this phenomenon, a series of experiments has been performed using a technique that provides direct observation of subband transitions between these two different types of *L* valleys. The results suggest that much improved midinfrared lasers can be fabricated using IV–VI semiconductor materials grown on (111)-oriented substrates.

PbSe/PbSrSe MQWs were grown on BaF₂(111) substrates in an Intevac GENII modular molecular-beam epitaxy (MBE) system. The MQW structures, with 15 periods, were directly deposited at 360 °C on a 150 nm BaF₂ buffer layer grown at 500 °C. PbSe quantum-well and PbSrSe barrier layer thickness were in the range of 5–30 and 25–40 nm, respectively. A 3% Sr-to-PbSe flux ratio was used for the growth of PbSrSe, resulting in about 7.5% Sr in the ternary alloy and a room temperature band gap of about 0.5 eV.¹¹ More detailed descriptions of PbSe/PbSrSe MQW growth on

^{a)}Electronic mail: huizhen@ou.edu

BaF₂(111) are described in Ref. 12. High-resolution x-ray diffraction (HRXRD) measurements of the MBE-grown MQW structures showed numerous satellite peaks and their spacings were used to calculate QW thicknesses.

A BioRad (FTS-60) FTIR spectrometer was used to measure transmission as a function of photon energy over a 700–6000 cm⁻¹ spectral range. The sample temperature was varied from 4.2 to 300 K. To suppress unwanted Fabry–Pérot interference fringes superposed on the FTIR transmission spectra, the top surface of the MQW samples was coated with a NiCr anti-interference film.¹³ The differential spectra are obtained by taking the difference between a transmission spectrum at one temperature and the spectrum at a slightly lower temperature. This takes advantage of the temperature dependence of the PbSe band gap, so that step edges associated with different transitions in the transmission spectra become peaks in the difference spectra. Thus the temperature difference spectra are in essence energy derivative spectra. The temperatures of the two transmission spectra were chosen so that the shift of the PbSe band gap was 1 meV. (Thus an energy resolution of 1 meV is maintained in this process.) For instance, the 293 K (4.2 K) differential spectrum was obtained by subtracting the 296 K (12 K) spectrum from a 293 K (4.2 K) spectrum. The variation in the temperature differences used in this procedure reflects the fact that the temperature dependence of the PbSe band gap is weaker at lower temperature. Another great advantage of the differential spectrum is that the differential process greatly reduces the residual Fabry–Pérot interference since the dielectric constant of the materials is very weakly dependent on temperature. This same technique, which enhances absorption features, has been used to study subband transitions in InSb quantum well structures.¹⁴

Figure 1 shows differential transmission spectra for a MQW sample with 20.6 nm thick PbSe QWs and 35 nm thick PbSrSe barriers for five different sample temperatures. The 4.2 K spectrum exhibits seven peaks. The highest energy peak at 405 meV is associated with the absorption edge of the PbSrSe barrier layers (the continuum), and the other six peaks are associated with subband transitions in the PbSe QWs. The lowest energy peak at 173 meV is due to the longitudinal (*l*) valley subband ($n=1$ valence band to $n=1$ conduction band) transitions, $(1-1)^l$, while the next peak at 180 meV is due to the threefold degenerate oblique (*o*) valley subband ($n=1$ valence band to $n=1$ conduction band) transitions $(1-1)^o$.

A comparison of the integrated intensities for the $(1-1)^l$ and $(1-1)^o$ peaks reflects the difference in the joint density of states between these two transitions. Identification of the other allowed $(2-2)^l$, $(2-2)^o$, $(3-3)^l$, and $(3-3)^o$ transitions marked in Fig. 1 is assisted by comparing integrated intensities of the differential peaks. In each case, peaks for *o*-valley transitions are stronger than those for *l*-valley transitions because of the larger transition matrix elements associated with the threefold degenerate oblique valleys.

As the temperature increases, all the subband and continuum transitions shift towards higher energies and peaks broaden due to increasing phonon scattering. At 210 K it is no longer possible to distinguish individual *l*-valley transitions from *o*-valley transitions in this sample.

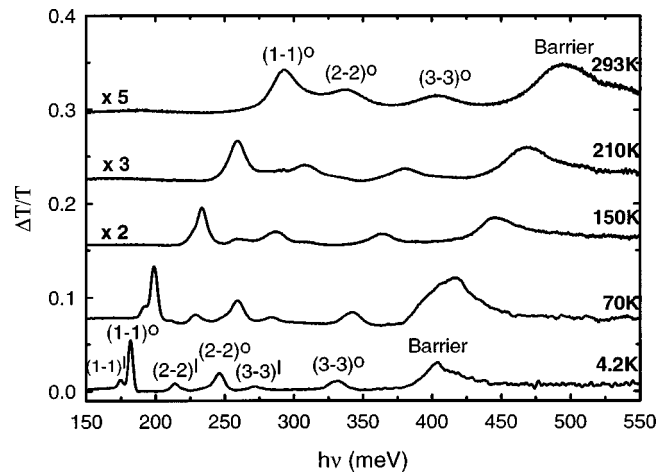


FIG. 1. FTIR differential transmission spectra measured at different temperatures from a PbSe/PbSrSe MQW sample with PbSe well width of 20.6 nm and PbSrSe barrier of 35 nm. Three longitudinal-valley subband transitions $(1-1)^l$, $(2-2)^l$, and $(3-3)^l$ and three oblique-valley subband transitions $(1-1)^o$, $(2-2)^o$, and $(3-3)^o$ are clearly seen.

Figure 2 shows differential transmission spectra for three MQW samples with different PbSe well widths. As the well width decreases from 29.7 to 9.7 nm, the splitting between the $(1-1)^l$ transition and the $(1-1)^o$ transition increases significantly, from 4 to 20 meV. As expected, the number of subbands involving both the *l* valley and *o* valley decrease from 4 to 2. Again, in all three samples the peak intensities of the *o*-valley transitions $(i-i)^o$, are stronger than their corresponding *l*-valley transitions, $(i-i)^l$, because of the threefold degeneracy of the oblique valleys.

Calculations for electron and hole subbands in IV–VI quantum wells have been carried out by Kriechbaum *et al.*,¹⁵ by Geist *et al.*¹⁶ and by Silva.¹⁷ In PbSe/PbEu(Sr, Mn)Se MQW systems the band alignment is type I for low Eu(Sr, Mn) concentrations. Assuming an equal band offset for conduction and valence band edge discontinuities ($\Delta E_c : \Delta E_v = 1:1$), and using the band structure parameters from Refs. 17 and 18, listed in Table I, and the barrier heights obtained from the measured FTIR transmission spectra, transition energies were calculated using the envelope

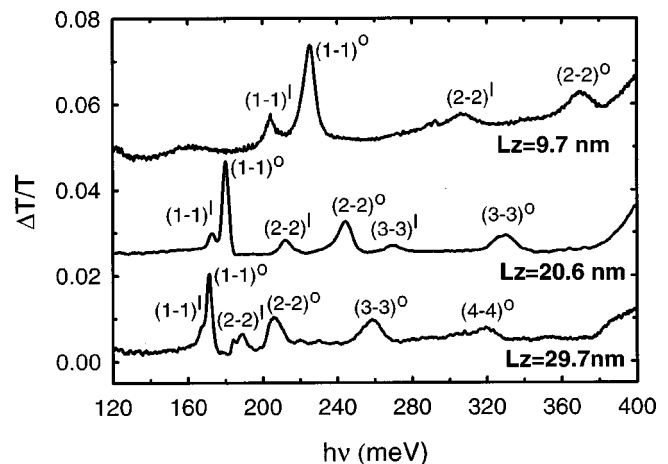


FIG. 2. FTIR differential transmission spectra for three MQW samples with well widths of 29.7, 20.6, and 9.7 nm, respectively. As the well width decreases $(i-i)^l$ and $(i-i)^o$ move towards higher energies and the number of confined states decreases.

TABLE I. Band structure parameters used in the calculations of quantized states of electrons and holes in PbSe/PbSrSe MQW structures. m_0 is the mass of a free electron.

	PbSe (4.2 K)	PbSrSe (4.2 K)	PbSe (295 K)	PbSrSe (295 K)
$m_e^l(m_0)$	0.070	0.070	0.113	0.113
$m_e^o(m_0)$	0.042	0.042	0.069	0.069
$m_h^l(m_0)$	0.068	0.068	0.108	0.108
$m_h^o(m_0)$	0.040	0.040	0.054	0.054
E_g (eV)	0.150	0.405	0.278	0.505

wave function approximation. Because of the small fraction of Sr in the barrier layers the electron and hole effective masses are assumed to be the same as those of PbSe in the calculations. The solid and dotted lines in Fig. 3 show the results of these calculations.

By comparing the calculations (lines) with the measured $(1-1)^l$ and $(1-1)^o$ transition energies at 4.2 and at 293 K shown in Fig. 3, it is clear that these calculations give a good description of the well width and temperature dependence for optical transitions in PbSe/PbSrSe MQW structures. In the room temperature differential transmission spectra, due to phonon-scattered broadening, longitudinal and oblique subband transitions could not be resolved, so the experimental points represent a mixture of ground state transitions from both l and o valleys.

The calculations presented in Fig. 3 consider only the quantum size effect, which is the dominant contribution in the case of PbSe/PbSrSe MQW structures. Strain-induced shifts of transition energies in the PbSe well layers are not considered here. The lattice mismatch between BaF₂(111) substrates and the epilayer is $\sim 1\%$ at room temperature. The epilayer thickness is $\sim 0.8 \mu\text{m}$. Thus it is expected that the PbSe/PbSrSe epilayers are completely relaxed with respect to BaF₂.¹⁹ There is a 0.18% lattice mismatch between the

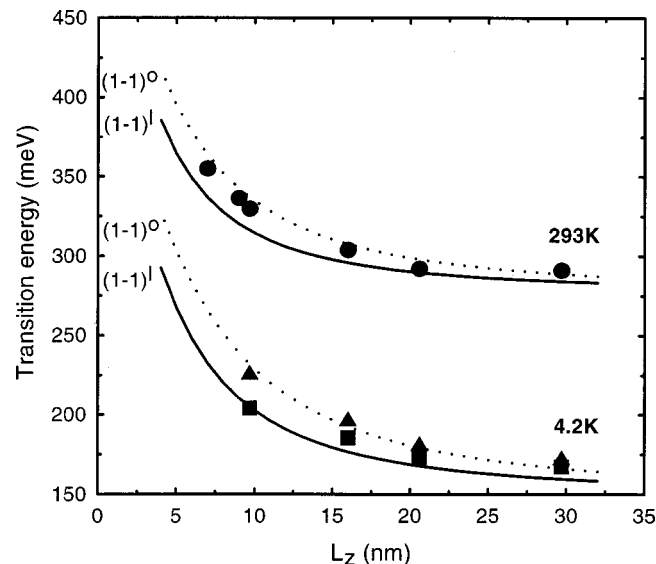


FIG. 3. Transition energies as a function of well width for PbSe/PbSrSe MQW structures at 4.2 and 293 K. Calculations are plotted as lines and experimental data from transmission measurements are plotted as symbols. ■: $(1-1)^l$ at 4.2 K, ▲: $(1-1)^o$ at 4.2 K, and ●: at room temperature.

PbSe well and the PbSrSe barrier materials, and this produces tensile strain in PbSe and compressive strain in PbSrSe. PbSe tensile strain is expected to cause additional splitting of the degeneracy of the longitudinal valley and oblique valleys on the order of a few meV.¹⁵ However, reliable shear deformation potential values for PbSe are not available so it was not possible to quantify this effect.

In summary, PbSe/PbSrSe (MQW) structures were grown on BaF₂(111) substrates by molecular-beam epitaxy. Longitudinal and oblique valley subband transitions from the MQW structures were unambiguously observed by Fourier transform infrared transmission spectroscopy without superposed interference fringes. The measured data of the quantum state transitions involving both valleys are in good agreement with calculations using the envelope wave function approximation. Although this investigation concerns the PbSe/PbSrSe MQW system, it provides a useful method by which to determine precisely electronic transitions in other IV–VI materials and heterostructures. The observed smaller joint density of states for longitudinal valleys shows that IV–VI quantum well lasers fabricated on (111)-oriented substrates should have lower threshold currents than similar devices fabricated on (100)-oriented substrates.

This work was supported by grants from the National Science Foundation (Grant Nos. DMR-9802396 and ECS-0080783).

¹Z. Feit, M. McDonald, R. J. Woods, V. Archambault, and P. Mak, Appl. Phys. Lett. **68**, 738 (1995).

²L. Partin, IEEE J. Quantum Electron. **QE-24**, 1716 (1988).

³Z. Shi, G. Xu, P. J. McCann, X. M. Fang, N. Dai, C. L. Felix, W. W. Bewley, I. Vurgaftman, and J. R. Meyer, Appl. Phys. Lett. **76**, 3688 (2000); Z. Shi, M. Tacke, A. Lambrecht, and H. Böttner, *ibid.* **66**, 2537 (1995).

⁴A. Fach, J. John, P. Müller, C. Paglino, and H. Zogg, J. Cryst. Growth **26**, 873 (1997).

⁵G. Bauer, M. Kriechbaum, Z. Shi, and M. Tacke, J. Nonlinear Opt. Phys. Mater. **4**, 283 (1995).

⁶P. J. McCann, S. Aanegola, and J. E. Furneaux, Appl. Phys. Lett. **65**, 2185 (1994).

⁷P. J. McCann, K. Namjou, and X. M. Fang, Appl. Phys. Lett. **75**, 3608 (1999).

⁸A. Ishida, S. Matsuura, M. Mizuno, and H. Fujiyasu, Appl. Phys. Lett. **51**, 478 (1987).

⁹S. Yuan, G. Springholz, G. Bauer, and M. Kriechbaum, Phys. Rev. B **49**, 5476 (1994); H. Krenn, S. Yuan, N. Frank, and G. Bauer, *ibid.* **57**, 2393 (1998).

¹⁰M. F. Khodr, P. J. McCann, and B. A. Mason, IEEE J. Quantum Electron. **32**, 236 (1996).

¹¹A. Lambrecht, N. Herres, B. Spanger, S. Kuhn, H. Böttner, M. Tacke, and J. Evers, J. Cryst. Growth **108**, 301 (1991).

¹²X. M. Fang, K. Namjou, I. Chao, P. J. McCann, N. Dai, and G. Tor, J. Vac. Sci. Technol. B **18**, 1720 (2000).

¹³S. W. McKnight, K. P. Stewart, H. D. Drew, and K. Moorjani, Infrared Phys. **27**, 327 (1987).

¹⁴N. Dai, F. Brown, P. Barsic, G. A. Khodaparast, R. E. Doezema, M. B. Johnson, S. J. Chung, K. J. Goldammer, and M. B. Santos, Appl. Phys. Lett. **73**, 1101 (1998).

¹⁵M. Kriechbaum, K. E. Ambrosch, E. J. Fantner, H. Clemens, and G. Bauer, Phys. Rev. B **30**, 3394 (1984); M. Kriechbaum, P. Koccevar, H. Pascher, and G. Bauer, IEEE J. Quantum Electron. **24**, 1727 (1988).

¹⁶F. Geist, H. Pascher, M. Kriechbaum, N. Frank, and G. Bauer, Phys. Rev. B **54**, 4820 (1996).

¹⁷A. de Andrada e Silva, Phys. Rev. B **60**, 8859 (1999).

¹⁸Landolt-Börnstein, in *Numerical Data and Functional Relationships in Science and Technology, Non-Tetrahedrally Bonded Compounds* Vol. 17 edited by O. Madelung (Springer, Berlin, 1987).

¹⁹J. W. Matthews and A. E. Blakeslee, J. Cryst. Growth **27**, 118 (1974).